

## THE ACS LCID PROJECT. X. THE STAR FORMATION HISTORY OF IC 1613: REVISITING THE OVER-COOLING PROBLEM<sup>1</sup>

EVAN D. SKILLMAN<sup>2</sup>, SEBASTIAN L. HIDALGO<sup>3,4</sup>, DANIEL R. WEISZ<sup>5,6,7</sup>, MATTEO MONELLI<sup>3,4</sup>, CARMEN GALLART<sup>3,4</sup>, ANTONIO APARICIO<sup>4,3</sup>, EDOUARD J. BERNARD<sup>8</sup>, MICHAEL BOYLAN-KOLCHIN<sup>9</sup>, SANTI CASSISI<sup>10</sup>, ANDREW A. COLE<sup>11</sup>, ANDREW E. DOLPHIN<sup>12</sup>, HENRY C. FERGUSON<sup>13</sup>, LUCIO MAYER<sup>14,15</sup>, JULIO F. NAVARRO<sup>16</sup>, PETER B. STETSON<sup>17</sup>, AND ELINE TOLSTOY<sup>18</sup>

*Draft version March 20, 2014*

### ABSTRACT

We present an analysis of the star formation history (SFH) of a field near the half light radius in the Local Group dwarf irregular galaxy IC 1613 based on deep *Hubble Space Telescope* Advanced Camera for Surveys imaging. Our observations reach the oldest main sequence turn-off, allowing a time resolution at the oldest ages of  $\sim 1$  Gyr. Our analysis shows that the SFH of the observed field in IC 1613 is consistent with being constant over the entire lifetime of the galaxy. These observations rule out an early dominant episode of star formation in IC 1613. We compare the SFH of IC 1613 with expectations from cosmological models. Since most of the mass is in place at early times for low mass halos, a naive expectation is that most of the star formation should have taken place at early times. Models in which star formation follows mass accretion result in too many stars formed early and gas mass fractions which are too low today (the “over-cooling problem”). The depth of the present photometry of IC 1613 shows that, at a resolution of  $\sim 1$  Gyr, the star formation rate is consistent with being constant, at even the earliest times, which is difficult to achieve in models where star formation follows mass assembly.

*Subject headings:* galaxies:dwarf, galaxies:evolution, galaxies:photometry, galaxies:stellar content, galaxies:structure, cosmology: early universe

### 1. INTRODUCTION

<sup>1</sup> Based on observations made with the NASA/ESA Hubble Space Telescope, obtained at the Space Telescope Science Institute, which is operated by the Association of Universities for Research in Astronomy, Inc., under NASA contract NAS 5-26555. These observations are associated with program #10505

<sup>2</sup> Minnesota Institute for Astrophysics, University of Minnesota, Minneapolis, MN, USA; skillman@astro.umn.edu

<sup>3</sup> Instituto de Astrofísica de Canarias. Vía Láctea s/n. E38200 - La Laguna, Tenerife, Canary Islands, Spain; shidalgo@iac.es, monelli@iac.es, carme@iac.es, aparicio@iac.es

<sup>4</sup> Department of Astrophysics, University of La Laguna. Vía Láctea s/n. E38200 - La Laguna, Tenerife, Canary Islands, Spain

<sup>5</sup> Astronomy Department, Box 351580, University of Washington, Seattle, WA, USA; dweisz@uw.edu

<sup>6</sup> Department of Astronomy, University of California at Santa Cruz, 1156 High Street, Santa Cruz, CA, 95064

<sup>7</sup> Hubble Fellow

<sup>8</sup> Institute for Astronomy, University of Edinburgh, Royal Observatory, Blackford Hill, Edinburgh EH9 3HJ, UK; ejb@roe.ac.uk

<sup>9</sup> Astronomy Department, University of Maryland, College Park, MD, USA; mbk@astro.umd.edu

<sup>10</sup> INAF-Osservatorio Astronomico di Collurania, Teramo, Italy; cassisi@oa-teramo.inaf.it

<sup>11</sup> School of Mathematics & Physics, University of Tasmania, Hobart, Tasmania, Australia; andrew.cole@utas.edu.au

<sup>12</sup> Raytheon; 1151 E. Hermans Rd., Tucson, AZ 85706, USA; adolphin@raytheon.com

<sup>13</sup> Space Telescope Science Institute, 3700 San Martin Drive, Baltimore, MD 21218, USA; ferguson@stsci.edu

<sup>14</sup> Institut für Theoretische Physik, University of Zurich, Zürich, Switzerland; lucio@physik.unizh.ch

<sup>15</sup> Department of Physics, Institut für Astronomie, ETH Zürich, Zürich, Switzerland; lucio@phys.ethz.ch

<sup>16</sup> Department of Physics and Astronomy, University of Victoria, BC V8P 5C2, Canada; jfn@uvic.ca

<sup>17</sup> Dominion Astrophysical Observatory, Herzberg Institute of Astrophysics, National Research Council, 5071 West Saanich Road, Victoria, British Columbia V9E 2E7, Canada; peter.stetson@nrc-cnrc.gc.ca

<sup>18</sup> Kapteyn Astronomical Institute, University of Groningen, Groningen, Netherlands; etolstoy@astro.rug.nl

### 1.1. Motivation

The present paper is part of the Local Cosmology from Isolated Dwarfs (LCID)<sup>19</sup> project. We have obtained deep *Hubble Space Telescope* (HST) photometry, reaching the oldest main sequence turn-off points, of six isolated dwarf galaxies in the Local Group: IC 1613, Leo A, Cetus, Tucana, LGS-3, and Phoenix. Five galaxies were observed with the Advanced Camera for Surveys (ACS, Ford et al. 1998), while Phoenix was observed with the Wide Field and Planetary Camera-2 (WFPC2, Holtzman et al. 1995). The main goal of the LCID project is to derive the star formation histories (SFHs), age-metallicity relations (AMRs), variable star populations, and stellar population gradients of this sample of galaxies. Our objective is to study their evolution at early epochs and to probe effects of cosmological processes, such as the cosmic UV background subsequent to the onset of star formation in the universe or physical processes such as the gas removal by supernovae (SNe) feedback. Our sample consists of field dwarfs which were chosen in an effort to study systems as free as possible from environmental effects due to strong interactions with a host, massive galaxy.

The SFH is a powerful tool to derive fundamental properties of dwarf galaxies and their evolution (Tolstoy et al. 2009), but to study the earliest epochs of star formation, deep CMDs, reaching the oldest main sequence turn-offs, are required (cf., Gallart et al. 2005). Our impressions of the evolution of dwarf galaxies are biased by studies of the nearby, gas-poor dSph companions of the Milky Way. Because of their proximity, deep CMDs are obtainable from ground-based observatories. In contrast,

<sup>19</sup> Local Cosmology from Isolated Dwarfs: <http://www.iac.es/project/LCID/>

the gas-rich, dIrr galaxies, which are found at greater distances, have few studies with comparable photometric depth. The Magellanic Clouds represent the one exception to this generalization, but, because of they are substantially more massive than the typical dwarf galaxy and have potentially complex histories due to their current interactions (see Kallivayalil et al. 2013, and references therein), they present less than ideal targets for study.

Because of the larger distances to the dIrrs, until the LCID project, none have had resolved star studies which reach down to the oldest main sequence turnoff stars. Thus, our view of the SFHs of dwarf irregular galaxies has been shaped by relatively indirect measures. The work by Gallagher et al. (1984) represents a seminal contribution to our understanding of the SFHs of dIrrs. Based on galaxy mass estimates, blue luminosities, and  $H\alpha$  luminosities, they demonstrated that most irregular galaxies were consistent with nearly constant star formation over their lifetimes (as opposed to the larger spiral galaxies which showed declining star formation rates, hereafter SFRs). Most importantly, they pointed out that “The constant SFR history implies that the simple classical model in which star formation is proportional to gas density in a closed system cannot be correct for irregular galaxies.” Modern observations of nearby dIrrs have been collected and summarized by Weisz et al. (2011), and indicate that, on average, SFRs are higher at early times, but that there are some dIrrs for which constant SFRs are a good approximation.

Recently, there have been theoretical papers emphasizing the difficulty in making models of galaxies which have nearly constant SFRs. Orban et al. (2008), Sawala et al. (2011), Weinmann et al. (2012), and Kuhlen et al. (2012) have all highlighted the difficulty of producing dwarf galaxies with properties comparable to those observed in the current universe. The degree of failure is greatest in the amount of mass converted into stars, which is of order one magnitude too large in cosmological simulations. This overproduction of stars in dwarfs is an extreme symptom of the “over-cooling problem” (c.f., Benson et al. 2003) faced by all galaxy modeling.

Without deep imaging of resolved stars in dIrr galaxies, we lack sufficient time resolution to study SFHs at the earliest times. For example, the earliest time bin used by Weisz et al. (2011) is 4 Gyr in duration. At this time resolution, we cannot distinguish between SFRs that are constant at all times, or SFRs that show considerable variation (most importantly evidence for an early dominant episode of SF). The initial time bin of 4 Gyr covers the time range from before re-ionization up to a redshift of  $\sim 2$  (which is approaching the peak of in the history of universal star formation, e.g., Madau et al. 1998), and represents this entire important range with a single average number. The observations of IC 1613 presented here resolve this initial period and represent a small step into this relatively unexplored territory.

### 1.2. *The Normal, Isolated, Low Mass, Dwarf Irregular Galaxy IC 1613*

Here we present our analysis of a deep HST/ACS observation of a field in IC 1613. As we discuss in section 3.1, the SFH that we derive for this field is likely a good representation for the entire galaxy. IC 1613 is a low-

luminosity, Local Group, dIrr galaxy which is one of the nearest gas-rich irregular galaxies (for a review of the properties of IC 1613 see van den Bergh 2000). Because of its proximity, IC 1613 offers the opportunity to reconstruct a detailed SFH of a relatively isolated and non-interacting dwarf irregular galaxy. IC 1613 also has very low foreground and internal reddening (although it lies within 5 degrees of the ecliptic). There have been several determinations of its distance based on Cepheid and RR Lyr variable stars and the tip of the red giant branch. Using all three methods, Dolphin et al. (2001) derived a distance of 730 kpc. In a comparison of all of the literature values (which included their own measurement using RR Lyrae and Cepheid data of 770 Kpc), Bernard et al. (2010) determine a mean distance of 760 kpc. The most recent determination is by Tammann et al. (2011) who derived a distance of 740 kpc using Cepheids. For consistency with the other LCID studies, we will adopt the distance estimate from Bernard et al. (2010) which corresponds to scales of  $221 \text{ pc arcminute}^{-1}$ ,  $3.7 \text{ pc arcsecond}^{-1}$ , and  $\sim 0.2 \text{ pc pixel}^{-1}$ .

IC 1613 is not considered to be a satellite of either the Milky Way or M31. Mateo (1998) included IC 1613 in the diffuse “Local Group Cloud,” and McConnachie (2012) determined a distance of 517 kpc and a velocity of  $-90 \text{ km s}^{-1}$  relative to the Local Group barycenter. As such, it is located very close to the zero velocity surface for M 31 and well within the zero velocity surface for the Local Group (McConnachie 2012). Given its isolated position and velocity, IC 1613 has not had any recent interactions, although interactions with other galaxies long ago cannot be ruled out. To date, there are no proper motion studies of IC 1613, which would be very valuable in determining its potential interaction history.

The physical parameters of IC 1613 were summarized in Cole et al. (1999). These properties are normal for an Im V galaxy with a moderate luminosity ( $M_V = -15.2$ ) and a small value of the maximum amplitude of the rotation curve ( $V_{max} = 25 \text{ km s}^{-1}$ ; Lake & Skillman 1989). Its SFR of  $0.003 M_\odot \text{ yr}^{-1}$  (Mateo 1998) is also normal for its type and luminosity. The most recent ISM oxygen abundance measurement was made by Lee et al. (2003), who obtained a spectrum where the  $\lambda 4363$  auroral line of [O III] was detected resulting in a measurement of  $12 + \log (\text{O}/\text{H}) = 7.62 \pm 0.05$ . This corresponds to 8.5% of the solar oxygen abundance (as determined by Asplund et al. 2009), which is slightly less than that of the SMC, and normal for a galaxy of its luminosity (e.g., Skillman et al. 1989; Berg et al. 2012). This combination of proximity and normality makes IC 1613 one of the best opportunities to study the properties of a dwarf star-forming galaxy that is relatively isolated (as is typical for Im V galaxies).

The overall structure of IC 1613 is also typical of an Im V galaxy. Ground-based studies have provided an overview of the stellar population distributions. Borissova et al. (2000) studied the distribution of luminous cool stars from J and K-band imaging and found AGB stars covering a wide range in age in all of their inner galaxy fields. Albert et al. (2000) conducted a wide field survey of IC 1613 for C and M stars, and found the (intermediate age) C stars extended out to 15 arcminutes, well beyond the regions where star formation

currently is active. Recently, Bernard et al. (2007) have conducted a wide field optical survey of IC 1613, and trace red giant branch (RGB) stars out to radii  $\geq 16.5$  arcminutes ( $\sim 3.6$  kpc), showing the galaxy to be more extended than previously thought.

The resolved stellar populations of IC 1613 have been studied with the HST twice in the past, both times using the WFPC2 camera. Cole et al. (1999) studied a central field and found IC 1613 to be a smoothly evolving galaxy with a relatively constant SFR over the last Gyr. Horizontal branch (HB) stars were detected, indicating the presence of an old population. Skillman et al. (2003a) obtained deep imaging for a field located 7.4 arcminutes southwest of the center. While that imaging was not quite deep enough to reach to the oldest main sequence turnoff stars, greatly limiting the time resolution at the oldest ages, the derived SFRs were constant within a factor of three over the entire lifetime of the galaxy.

In this paper, we present the SFH of IC 1613 obtained from observations with the ACS on the HST. The photometry reaches the oldest main sequence turn-offs of the galaxy, allowing us to obtain an accurate SFH even for the oldest stellar populations. Bernard et al. (2010) have already used these observations to conduct a study of the variable star content of IC 1613.

The structure of the paper is as follows: in §2 the observations and data reduction are discussed and the CMD is presented. The derived SFH of IC 1613 is presented in §3 and is compared with those of other LCID galaxies in §4. The implications of the SFH of IC 1613 for galaxy modeling, and, in particular, the over-cooling problem are discussed in §5. The main conclusions of the work are summarized in §6. As with the previous LCID papers, cosmological parameters of  $H_0 = 70.5 \text{ km s}^{-1} \text{ Mpc}^{-1}$ ,  $\Omega_m = 0.273$ , and a flat Universe with  $\Omega_\Lambda = 1 - \Omega_m$  are assumed (i.e., Komatsu et al. 2009).

## 2. OBSERVATIONS AND DATA REDUCTION

The ACS observations of IC 1613 were obtained between August 18 and 20, 2006. The F475W and F814W bands were selected as the most efficient combination to trace age differences at old ages, since they provide the smallest relative error in age and metallicity in the main-sequence and sub-giant regions (see C. Gallart et al. 2013, in prep). Total integration times were 31,489 s in F475W and 27,119 s in F814W. The observations were organized into 12 visits of 2 orbits each, and each orbit was split into one F475W and one F814W exposure (in order to maximize sampling of variable star light curves). The observing log is reported in Bernard et al. (2010). Dithers of a few pixels between exposures were introduced to minimize the impact of pixel-to-pixel sensitivity variations (“hot pixels”) in the CCDs. The observed field of IC 1613 is shown in Figure 1. At the adopted distance to IC 1613, the footprint of the ACS covers  $0.56 \text{ kpc}^2$ . The optical scale length of IC 1613 is  $2'.9$  (Bernard et al. 2007) and the stellar distribution can be traced out beyond 15 arcminutes, so the  $3'.4 \times 3'.4$  format of the ACS covers only a fraction of the area of IC 1613 ( $\sim 9\%$ ).

We analyzed the images taken directly from the STScI pipeline (bias, flat-field, and image distortion corrected). Two PSF-fitting photometry packages, DAOPHOT/ALLFRAME (Stetson 1994) and

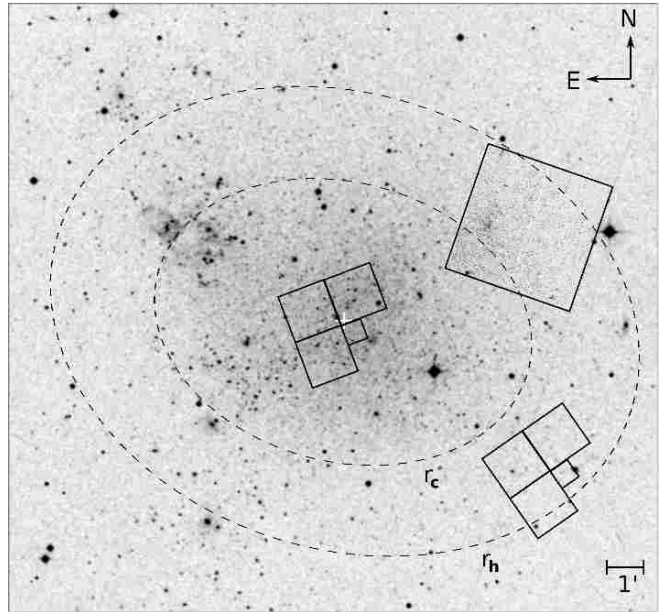


FIG. 1.— The location of the newly observed HST ACS field in IC 1613 (rectangle, upper right). The optical center of the galaxy is indicated by the white cross. The two dashed ellipses correspond to the core radius ( $r_c$ ) at  $4'.5$  ( $\sim 1.0$  kpc) and the half-light radius ( $r_h$ ) at  $6'.5$  ( $\sim 1.4$  kpc). As can be seen from the figure, the HST ACS field is located between the two. Also indicated are the positions of the two previous HST WFPC2 fields (chevrons) from Cole et al. (1999) (inner) and Skillman et al. (2003a) (outer).

DOLPHOT (Dolphin 2000), were used independently to obtain the photometry of the resolved stars. Non-stellar objects and stars with discrepant and large uncertainties were rejected based on estimations of profile sharpness and goodness of fit. See Monelli et al. (2010b) for more details about the photometry reduction procedures. Individual photometry catalogs were calibrated using the equations provided by Sirianni et al. (2005). The zero-point differences between the two sets of photometry are small ( $\lesssim 0.04$  mag) and typical for obtaining HST photometry with different methods (Hill et al. 1998; Holtzman et al. 2006). We direct the reader to extensive photometry reduction comparisons of LCID observations discussed in Monelli et al. (2010b) and Hidalgo et al. (2011). For simplicity, the rest of this paper is based on only the DOLPHOT photometry dataset which contains 165,572 stars.

Signal-to-noise limitations, detector defects, and stellar crowding can all impact the quality of the photometry of resolved stars with the resulting loss of stars, changes in measured stellar colors and magnitudes, and systematic uncertainties. To characterize these observational effects, we injected  $\sim 5 \times 10^5$  artificial stars in the observed images and obtained their photometry in an identical manner as for the real stars. Monelli et al. (2010b) and Hidalgo et al. (2011) provide detailed descriptions of the procedures we adopt for the characterization and simulation of these observational effects.

The CMD of IC 1613 is shown in Figure 2. Individual stars are plotted in the left panel and density levels are shown in the right panel. The left axis shows magnitudes in the ACS photometric system corrected for extinction. Absolute magnitudes are given on the right axis using the adopted values for the distance modulus

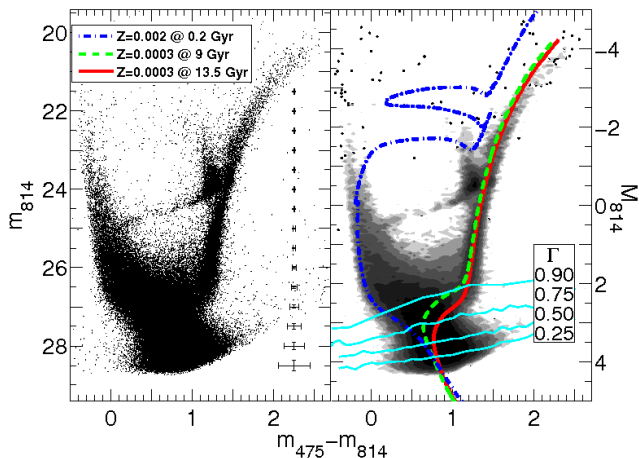


FIG. 2.— The HST/ACS color-magnitude diagram of IC 1613 based on 165,572 stars. In the left panel, individual stars are plotted while the right panel shows star density levels. Star densities bordering the plotted levels run from 8 to 512 stars  $\text{dmag}^{-2}$ , evenly spaced by factors of 2. The left axis shows observed magnitudes corrected for extinction. The right axis shows absolute magnitudes. A distance modulus of  $(m - M)_0 = 24.40$  and an extinction  $A_{F475W} = 0.094$ ,  $A_{F814W} = 0.047$  have been used. The lines across the bottom of the right panel show the 0.25, 0.50, 0.75 and 0.90 completeness levels. Three isochrones from the BaSTI stellar evolution library have been over plotted for comparison.

$(m - M)_0 = 24.40$ ) and extinctions ( $A_{F475W} = 0.094$  and  $A_{F814W} = 0.047$  mag) from Bernard et al. (2010). The completeness factor,  $\Gamma$ , the rate of recovered artificial stars as a function of magnitude and color, is shown in Figure 2, right panel, at  $\Gamma = 0.25, 0.50, 0.75$  and  $0.90$ . Finally, in order to highlight the main features of the CMD, three isochrones from the BaSTI stellar evolution library (Pietrinferni et al. 2004) are also shown in the right panel as labeled in the inset.

As shown in Figure 2, our photometry reaches below the oldest main-sequence turn-off at the 50% completeness limit, allowing for very strong constraints on the oldest epochs of star formation. These observations are  $\sim 1.5$  mag fainter than the deepest CMD previously obtained for this galaxy (Skillman et al. 2003a). Since there are no early isolated episodes of elevated SFR in the SFH, there is no obvious indication of the time resolution in the early SFH of IC 1613 shown in Figure 2. However, extensive modeling with similar LCID datasets has shown that observations of this quality yield a time resolution of  $\sim 1$  Gyr (Monelli et al. 2010b,c; Hidalgo et al. 2011).

Consistent with earlier observations, a comparison of the observations with the over-plotted isochrones and the presence of an extended horizontal branch indicate that a very old, very low metallicity stellar population is present in the galaxy. The gap produced in the HB by the RR-Lyrae variables and a red clump (RC) at the red end of the HB are clearly defined. An MS with stars younger than 200 Myr is clearly apparent. Some blue and red core helium-burning stars might also be present above the RC ( $m_{814} < 22.4$ ;  $0.5 < (m_{475} - m_{814}) < 1.2$ ). The RGB bump can be also observed at  $(m_{475} - m_{814}) \sim 1.4$  and  $m_{814} \sim 23.1$  mag; this broad feature can be explained by an extended SFH (Monelli et al. 2010a).

### 3. THE SFH OF IC 1613

#### 3.1. A Representative Field

As can be seen from Figure 1, the HST ACS field of view covers only a small fraction of IC 1613 ( $\sim 9\%$ ). The position of the field was chosen mainly as a balance between optimizing the number of stars but minimizing the effects of crowding at the photometric limit. However, the resulting position lies just inside of the half-light radius of IC 1613, which is quite fortunate.

Ideally, we would like to characterize the global SFH of IC 1613 from the observed field. Stellar population gradients are universal in dwarf galaxies and have been observed over a wide range of physical characteristics (Dohm-Palmer et al. 1997; Gallagher et al. 1998; Tolstoy et al. 1998; Dohm-Palmer et al. 1998; Battinelli & Demers 2000; Aparicio et al. 2000; Aparicio & Tikhonov 2000; Hidalgo et al. 2003; Magrini et al. 2003; Leisy et al. 2005; Battinelli & Demers 2006; Demers et al. 2006; Hidalgo et al. 2008; Gallart et al. 2008; Noël et al. 2009; Ryś et al. 2011; Grocholski et al. 2012). In all cases, the gradients are in the sense that the mean age of the stellar population is younger toward the center of the galaxy (see discussion in Hidalgo et al. 2013, for further details).

Since the observed field is close to the half-light radius, we make a type of “mean value” assumption and assume that the SFH derived from the observed field is a relatively good representation of the global SFH for IC 1613. The balance between outer fields (with relatively more older stars) and inner fields (with relatively more younger stars) should not be too different from the SFH of a field at the half-light radius. For the rest of the paper the discussion will be based on this assumption and the SFH history of the observed field and the global SFH of IC 1613 will be used interchangeably. This assumption is supported by the comparison of HST observations of IC 1613 from different fields presented in §3.4. Note that our main result, the absence of a dominant star formation episode at early times, would only strengthen by the addition of more younger stars at smaller radii. The opposite possibility (a relative surplus of older stars in the inner parts of the galaxy) is constrained by the direct observation of the number of RGB stars in the central field from the earlier HST/WFPC2 observations (Cole et al. 1999, see discussion in section §3.4).

#### 3.2. Main Features of the SFH of IC 1613

Following the other LCID studies, we first use the IAC method, consisting of IAC-star (Aparicio & Gallart 2004), IAC-pop (Aparicio & Hidalgo 2009), and MiniIAC (Aparicio & Hidalgo 2009; Hidalgo et al. 2011) in order to solve for the SFH and AMR. Details of the methodology can be found in Hidalgo et al. (2011). Specifically, the solution has been obtained using the BaSTI (Pietrinferni et al. 2004) stellar evolutionary libraries and the bolometric corrections of Bedin et al. (2005), and the uncertainties are the statistical uncertainties and do not include certain systematics (e.g., the use of a different stellar library).

Figure 3 shows a plot of the SFH of IC 1613,  $\psi(t, Z)$ , as a function of both  $t$  and  $Z$ .  $\psi(t)$  and  $\psi(Z)$  are also shown in the  $\psi - t$  and  $\psi - Z$  planes, respectively. The projection of  $\psi(t, Z)$  on the age-metallicity plane shows the AMR, including the metallicity dispersion.

Figure 3 shows the presence of star formation at all times, and the gradual build up of metallicity with time. Note especially the relatively constant SFR over the first

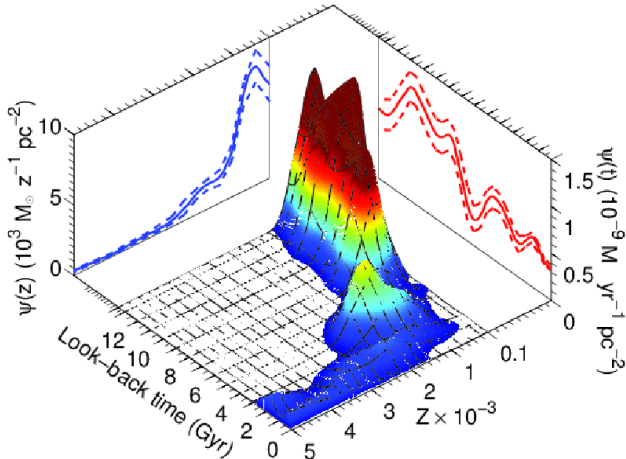


FIG. 3.— Star formation history,  $\psi(Z, t)$ , of IC 1613 derived as described in the text. The SFH as a function of age  $\psi(t)$  and metallicity  $\psi(Z)$  are shown projected on the  $\psi$ –time and  $\psi$ –metallicity planes, respectively. Dashed lines give the statistical error intervals. The age–metallicity relationship is the projection onto the look-back time–metallicity plane.

6 Gyr of the history of IC 1613 (variations of  $\sim 30\%$  or less in SFR). While the IAC-pop solution suggests a slight (factor of 2) decrease in average SFR about 8 Gyr ago ( $z \approx 1$ ), there is no evidence for a dominant episode of star formation before the end of reionization ( $\sim 12.8$  Gyr, or  $z \approx 6$ , Fan et al. 2006) or around the age of the peak SFR density of the universe ( $\sim 10$  Gyr, or  $z \approx 2$ , Hopkins 2004)). We emphasize that there is no evidence of a dominant episode of star formation in very early times (lookback time  $\geq 11$  Gyr), despite our ability to resolve such a feature.

In Figure 4 we show  $\psi(t)$ , the AMR (with their associated errors), and the cumulative stellar mass fraction of IC 1613, as a function of time. Three vertical dashed lines show the ages of the 10th, 50th, and 95th-percentile of the integral of  $\psi(t)$ .

The main features of the SFH of IC 1613 are nearly continuous star formation and an accompanying smooth increase in the stellar metallicity. The SFR varies by at most a factor of two from its mean value over the entire lifetime of the galaxy. Most importantly, there is no strong initial epoch of star formation, as is seen in the LCID dSph galaxies and transition (dSph/dIrr) galaxies. This is reflected in the cumulative stellar mass fraction plot which is close to the diagonal line of a constant SFR.

Figure 5 shows the observed CMD, the best-fit CMD, and the corresponding residuals. Residuals are given in units of Poisson uncertainties, obtained as  $(n_i^o - n_i^c)/\sqrt{n_i^c}$ , where  $n_i^o$  and  $n_i^c$  are the number of stars in bin  $i$  of an uniform grid defined on the observed and calculated CMDs, respectively. Because the solution is heavily determined by the main sequence stars (i.e., the RGB and HB stars are not used in the solution, see discussion in Hidalgo et al. 2013), the residuals along the MS are negligible. There are significant residuals at the faintest levels (where the incompleteness is large) and in the horizontal branch (which is typically not well fit by models).

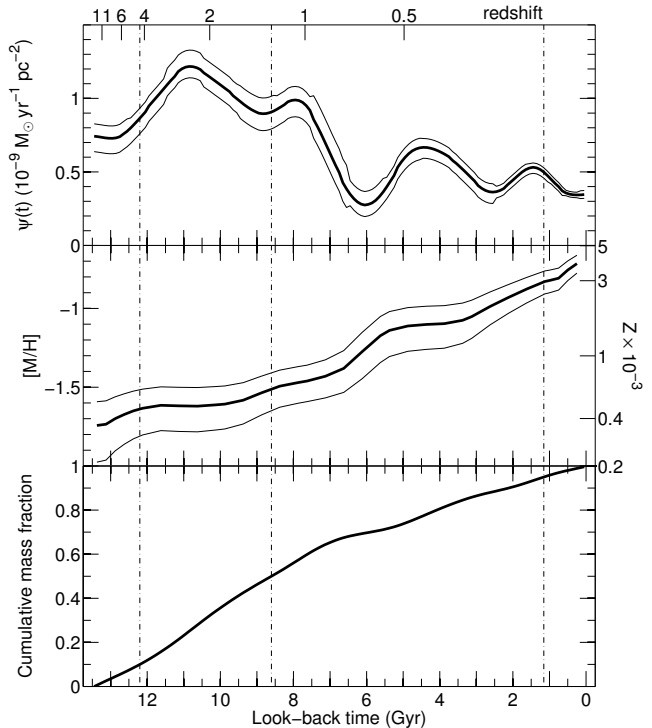


FIG. 4.— Star formation rate,  $\psi(t)$  (upper panel), metallicity (middle panel), and cumulative stellar mass fraction (lower panel) of IC 1613. Thin lines give the uncertainties. Vertical dotted-dashed lines indicate the times corresponding to the 10<sup>th</sup>, 50<sup>th</sup> and 95<sup>th</sup> percentiles of  $\psi(t)$ , i.e., the times for which the cumulative fraction of mass converted into stars was 0.1, 0.5 and 0.95 of the current total. The cumulative total mass of stars formed is  $5.33 \pm 0.10 \times 10^6 M_\odot$ . The mean metallicity,  $\langle [M/H] \rangle$ , is  $-1.3 \pm 0.1$ . The average star formation rate,  $\langle \psi(t) \rangle$ , is  $0.081 \pm 0.001 M_\odot \text{yr}^{-1}$ . A redshift scale is given in the upper axis.

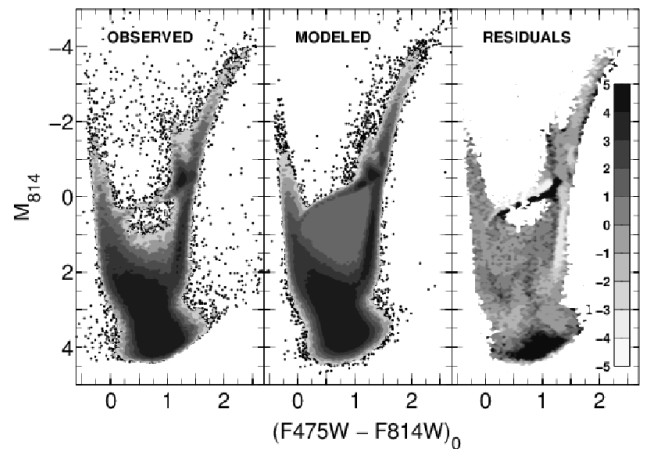


FIG. 5.— Observed (left panel), calculated model (central panel), and residual (right panel) CMDs. The calculated CMD has been built using IAC-star with the solution SFH of IC 1613 as input. The grey scale and dot criteria for the first two is the same as for Figure 2. The residuals are in units of Poisson uncertainties.

### 3.3. Comparison of SFHs Derived with Different Methods

As for the other galaxies in the LCID sample, we have obtained the SFH of IC 1613 using the MATCH (Dolphin 2002) and Cole (Skillman et al. 2003a) methods in

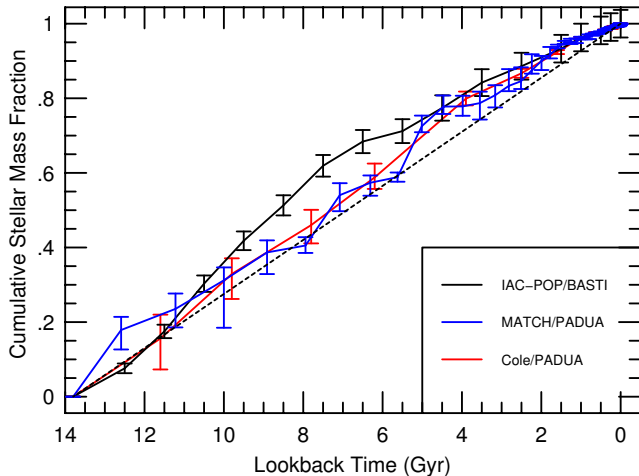


FIG. 6.— Cumulative stellar mass fraction as a function of lookback time of the solutions obtained for IC 1613 with different methods, indicated in the label. IAC-Pop corresponds to the solution obtained with IAC-star/MinnIAC/IAC-pop using the BaSTI stellar evolution library. Cole and Match methods make use of the Girardi et al. (2010) stellar evolution library.

addition to the IAC method. These two methods use Girardi et al. (2010) for the stellar evolution library for this comparison (for a description of the main features of these methods and the particulars of their application to LCID galaxies, see Monelli et al. 2010b). In this exercise, we have allowed all parameters (e.g., distance, reddening, etc.) to be solved for optimally independently. That is, we are not trying to compare codes, but rather, trying to make an assessment of the systematic errors that may arise due to choices of different stellar libraries, codes, etc.

There are three main sources of uncertainties in deriving SFHs (see, e.g., discussion in Aparicio & Hidalgo 2009): the input observational uncertainties, the statistical uncertainties of the solution, and the systematic uncertainty of the limitations of our knowledge of stellar evolution. In a specific test of creating synthetic photometry from one stellar library and using a different stellar library to derive a SFH, Aparicio & Hidalgo (2009) showed that the uncertainties associated with our knowledge of stellar evolution dominated those of the numerical methodology or the observation uncertainties. They recommend always using more than one stellar evolution library when analyzing a real population to test for these effects. Weisz et al. (2011) and Dolphin (2012) have also shown that, for sufficiently deep photometry, the stellar evolution uncertainties, as approximated by differences between stellar evolution model and their resulting libraries, represent the dominant systematic uncertainty for derived SFHs. (See also the discussion in Dotter et al. 2007, concerning the effects of varying heavy element abundance patterns.)

Thus, using different stellar libraries is integral to this comparison. The SFH derived using MATCH features uncertainties calculated following the prescriptions in Dolphin (2013). In this case, random uncertainties were generated using a hybrid Monte Carlo (HMC) process (Duane et al. 1987), with implementation details as described by Dolphin (2013). The result of this Markov Chain Monte Carlo routine is a sample of 10,000 SFHs

whose density is proportional to the probability density. (That is, the density of samples is highest near the maximum likelihood point.) Upper and lower random error bars for any given value (e.g., cumulative stellar mass fraction at a particular point in time) are calculated by identifying the boundaries of the highest-density region containing 68% of the samples, with the value 68% adopted as it is the percentage of a normal distribution falling between the  $\pm 1 \sigma$  bounds.

Figure 6 shows the cumulative stellar mass fraction of IC 1613 as obtained with the three different methods. The agreement between the three methods is very good and all three are best described as consistent with nearly constant star formation. The one small difference between the SFHs is the offset at intermediate ages between the solution based on the BASTI models and the two based on the Padua models. A comparison using the same code with two different stellar libraries shows that about half of this difference is due to the differences between the stellar libraries (which have differences in physical inputs and differ in the treatment of core convective overshoot during the central H burning stage) and the other half is likely attributable to how different sections of the CMD are binned and weighted.

This comparison strongly supports the conclusion that the star formation in IC 1613 has been relatively constant for the lifetime of the galaxy. The similar behavior of the three solutions allows us to be confident that our conclusions are independent of the stellar evolution libraries and SFH solution method. Most importantly, an early dominant star formation event is clearly ruled out.

Note also that IC 1613 has clearly formed the vast majority of its stars after the epoch of reionization which occurred in the first Gyr of the history of the universe (cf. Fan et al. 2006).

#### 3.4. Comparison of SFHs Derived from Other HST Observations of IC 1613

Relatively deep imaging of IC 1613 has been obtained with the HST three times: a central field obtained with the WFPC2 camera (9 orbits) with a depth in I-band of  $\sim 26.5$  mag. presented by Cole et al. (1999), a deep (24 orbits) outer field (radius  $\approx 1.4$  kpc) obtained with the WFPC2 camera with a depth in I-band of  $\sim 27.3$  presented by Skillman et al. (2003a), and our new imaging of an outer field (radius  $\approx 1.2$  kpc) obtained with the ACS camera with a depth in I-band of  $\sim 28.7$ . Figure 7 presents a comparison of the photometry for these three observations. In making Figure 7, identical quality cuts were made on the data, so that they are directly comparable (although the WFPC observations were obtained with an F555W filter and the present ACS observations were obtained with an F475W filter).

Figure 8 shows the cumulative stellar mass fraction of IC 1613 as obtained from the three different observations. The SFHs for the WFPC2 fields are newly derived from the archival data (Dolphin et al. 2005; Weisz et al. 2014). All three SFHs were obtained using the MATCH code (Dolphin 2002) and the Padua (Girardi et al. 2010) stellar evolution library. The errorbars were derived following the prescription outlined in Dolphin (2013).

This comparison to SFHs derived from shallower data needs to be approached carefully. Clearly, the larger uncertainties inherent in the shallower observations are re-

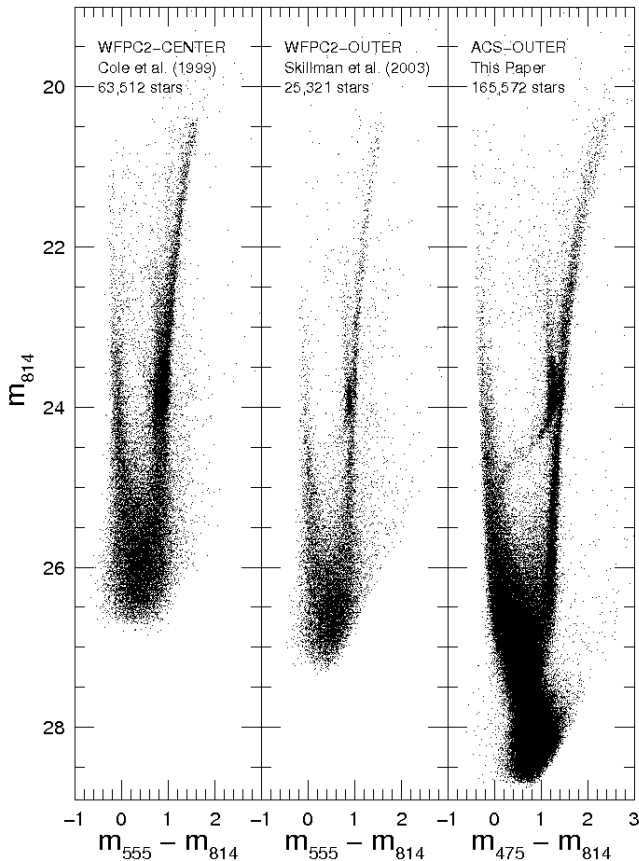


FIG. 7.— Comparison of the photometry obtained for IC 1613 from three different fields observed with the HST. WFCP2-CENTER corresponds to the 9 orbit observation presented in Cole et al. (1999), WFCP2-OUTER corresponds to the 24 orbit observation presented in Skillman et al. (2003a), and ACS-OUTER corresponds to the new ACS observations presented here.

flected by larger errorbars on the individual points. However, since the dominant component of the uncertainties are systematic, and since these can only be estimated and not calculated directly, these should be interpreted as “best estimates”. Predicting early SFHs from photometry which does not reach the oldest main sequence turn-offs is vulnerable to systematic biases. There is no substitute for the deep observations with the resulting strong constraints on the old age SFH. Nonetheless, this comparison allows us to test our assumption of the representative nature of the ACS observation for the global SFH of IC 1613.

The main impression from Figure 8 is that the SFHs for all three observations are best described as consistent with nearly constant star formation, but only the deeper ACS observations clearly rule out a dominant episode of early star formation. Thus, Figure 8 does provide strong support for the assumption that the SFH derived from the ACS observations can be assumed to be representative of the global SFH for IC 1613. Given the caveats from the previous paragraph we will refrain from any further discussion of this comparison.

#### 4. THE SFH OF IC 1613 COMPARED TO OTHER LCID GALAXIES

In this section, we will compare the SFH of IC 1613 with that of Leo A (the other dIrr galaxy of the LCID

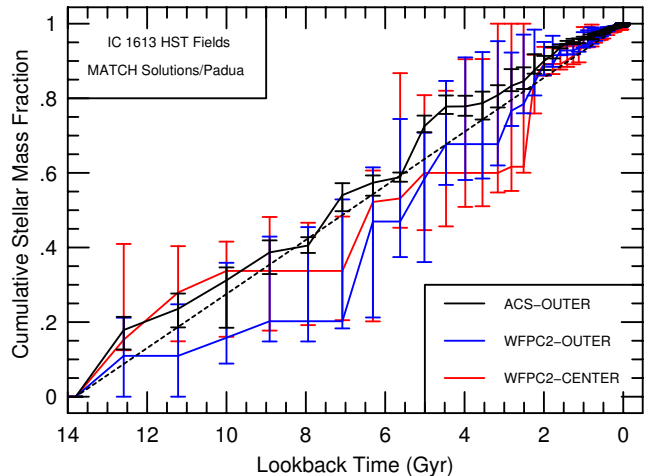


FIG. 8.— Cumulative stellar mass fraction as a function of lookback time of the solutions obtained for IC 1613 from three different fields observed with the HST. All three solutions were derived with MATCH using the Girardi et al. (2010) stellar evolution library. The errorbars were derived following the prescription outlined in Dolphin (2013). As in Figure 7, WFCP2-CENTER corresponds to the 9 orbit observation presented in Cole et al. (1999), WFCP2-OUTER corresponds to the 24 orbit observation presented in Skillman et al. (2003a), and ACS-OUTER corresponds to new ACS observations presented here. Note that the deeper ACS observations have allowed significantly smaller uncertainties at the earliest times. All three SFHs are consistent with a constant SFR over the lifetime of the galaxy, but only the deeper ACS observations clearly rule out a dominant episode of early star formation.

sample, Cole et al. 2007), Phoenix and LGS-3 (the two dSph/dIrr transition galaxies, Hidalgo et al. 2009, 2011) and with those of Cetus and Tucana (the two dSphs, Monelli et al. 2010b,c). Note that the LCID sample covers a range in dynamical masses. From Kirby et al. (2014) the dynamical masses of IC 1613, Leo A, LGS-3, Cetus, and Tucana are:  $1.1 \pm 0.2 \times 10^8 M_{\odot}$ ,  $1.5^{+0.6}_{-0.5} \times 10^7 M_{\odot}$ ,  $2.7^{+3.7}_{-2.0} \times 10^7 M_{\odot}$ ,  $4.0^{+1.0}_{-0.9} \times 10^7 M_{\odot}$ , and  $7.1 \pm 1.2 \times 10^7 M_{\odot}$ , respectively. For Phoenix, we derive a value of  $\sim 2.7 \times 10^7 M_{\odot}$ , assuming a velocity dispersion of  $\sim 8 \text{ km s}^{-1}$  (Zaggia et al. 2011) and a half-light radius of 454 pc (McConnachie 2012).

Figure 9 compares the SFH and the AMR of IC 1613 with the other LCID galaxies. In the top panel of Figure 9, the SFRs ( $\Psi_{norm}$ ) have been normalized such that the area under each curve is 1 (i.e., the integral of the SFR over the lifetime of the galaxy is 1). The differences between the SFHs as a function of morphological type is quite remarkable. Both dIrr galaxies lack the dominant initial episode of star formation seen in both the dSph and transition type galaxies. Although the SFHs are the main topic of this study, the AMRs are also solved for in deriving the SFHs and are included here for completeness. Both dIrr galaxies also show relatively little metal enrichment during the first  $\sim 6$  Gyr, with gradual enrichment following.

Note that Hidalgo et al. (2011) highlighted the lack of early chemical enrichment in the transition galaxy LGS-3 and hypothesized that the differences between the transition galaxies and dSphs (which show early chemical enrichment) might be understood if the dSphs were initially more massive systems than the transition galaxies. Under this hypothesis, the delayed metal enrichment in the

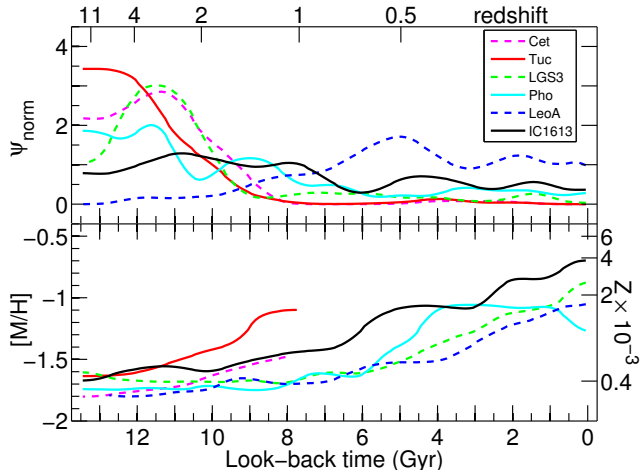


FIG. 9.— Comparison between the SFHs and the AMRs of IC 1613 (this paper) and the other LCID galaxies. A redshift scale is given on the top axis.

transition galaxies is due to higher losses of metals during times of higher SFRs for the lower mass transition galaxies. In this light, it is interesting that IC 1613 (and also Leo A) show delayed metal enrichment, but with no initial high SFR. In this regard, further comparisons of the SFH and AMRs of transition galaxies and dIrr galaxies would be of great interest<sup>20</sup>.

Before comparing to theoretical models, we introduce one last comparative figure. In Figure 10, we show a comparison between the SFHs of the six LCID galaxies as cumulative stellar mass fractions. In the upper panel, only the statistical uncertainties are shown. In the lower panel, the systematic uncertainties are included following the methodology of Dolphin (2013). Because all of the LCID galaxies have been observed to comparable depth, systematics in the models should have similar impacts to all of the galaxies. Thus, it is likely appropriate to make comparisons using the upper panel. Nonetheless, the lower panel shows the larger uncertainties encountered when trying to account for systematics and, even with the larger uncertainties, the six galaxies are shown to each have distinctive features in their SFHs.

Portraying the SFHs as cumulative stellar mass fractions (as opposed to SFR as a function of time) is the optimal way to compare observations to theoretical models for several reasons. Variations in observed SFRs can be strongly affected by time binning and the changing time resolution as a function of lookback time. Often, it is possible to have very different impressions of a single SFH simply by changing the time binning. It is possible to match the observational time binning by reducing the

<sup>20</sup> It is important to note that the definition and nature of transition galaxies is not a completely settled issue. Clearly, many transition galaxies are low mass dIrrs lacking H II regions simply due to a gap in recent massive star formation as noted by Skillman et al. (2003b). A nearby example of a galaxy with all of the properties of a dIrr that has been labeled a transition galaxy is Pegasus (Skillman et al. 1997). Weisz et al. (2011) hypothesize that the majority of transition galaxies are simply lower mass dIrrs (supported by the recent study of Leo T, Weisz et al. 2012), but with a sub-sample of very gas poor galaxies like Phoenix (Young et al. 2007). If Phoenix and LGS-3 are not representative of the typical transition galaxy, then this point needs to be explored further before generalizations can be made about the true nature of the transition galaxies.

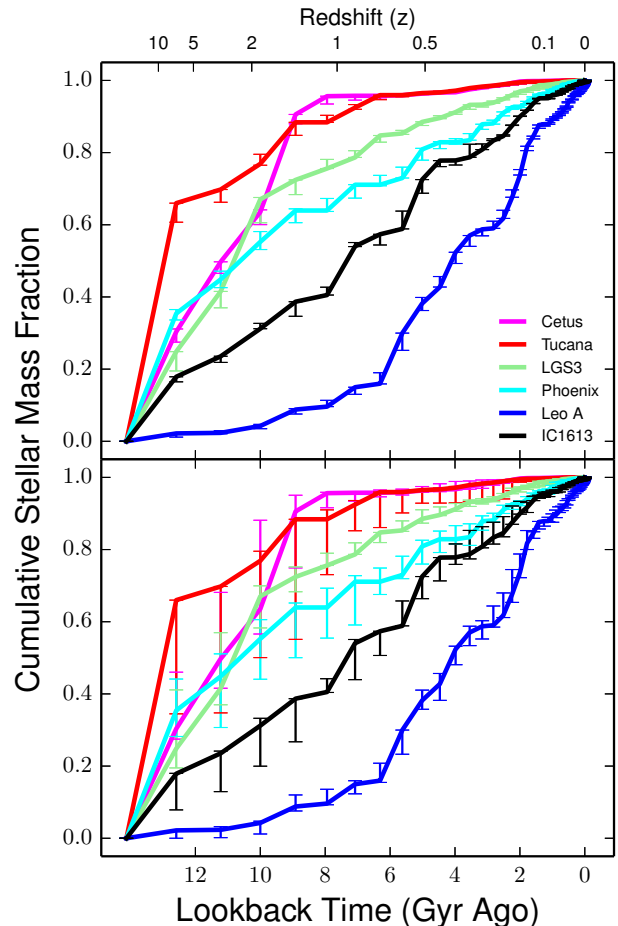


FIG. 10.— Comparison between the SFHs of the LCID galaxies shown as cumulative stellar mass fraction. The upper panel shows only the statistical uncertainties. The lower panel accounts for estimated systematic uncertainties as discussed in (Dolphin 2012, 2013). A redshift scale is given on the top axis.

resolution in the models, but using the cumulative stellar mass fraction as the diagnostic avoids this problem altogether. It is also possible to compare galaxies at any arbitrary value of the cumulative stellar mass fraction, as opposed to choosing particular values to focus on. In the comparisons that follow, we will use the cumulative stellar mass fraction as the sole diagnostic. Note that there is one obvious failing of the cumulative stellar mass fraction as the sole diagnostic, and that is the lack of information about the absolute masses of the systems. In the following comparisons, we will provide information about the masses of both the observed and modeled systems.

## 5. THE EARLY EVOLUTION OF IC 1613 AND THE OVER-COOLING PROBLEM

### 5.1. Background

Recently, Orban et al. (2008), Sawala et al. (2011), Weinmann et al. (2012), and Kuhlen et al. (2012) have all highlighted the difficulty of producing dwarf galaxies in simulations with properties comparable to those observed in the current universe. Together, the introductions to their papers give a comprehensive overview of the problems with modeling dwarf galaxy evolution.

To summarize, there are two major problems. The first problem is the observed abundance of low-mass galaxies.

The observed slope of the low-mass galaxy luminosity function is shallow relative to the slope of the halo mass function and this difference seems to be a result of an extreme inefficiency of galaxy-scale star formation over cosmic times. The well known problem of “the missing satellites” (Kauffmann et al. 1993; Klypin et al. 1999; Moore et al. 1999) is one manifestation of this problem at very low luminosities/halo masses.

The second problem relates to *when* stars are formed in galaxies. A natural assumption is that the time-scale for global star formation is related to the time-scale of baryonic accretion onto galaxies. However, low-mass halos assemble almost all of their (dark matter) mass at high redshift (e.g., Fakhouri et al. 2010), while essentially all field dwarf galaxies show star formation continuing to the present day (e.g., Weisz et al. 2011). IC 1613 and Leo A are extreme examples of this, with essentially a constant SF rate across cosmic time for IC 1613 and delayed star formation in the case of Leo A.

In order to suppress the abundance of low-mass galaxies, most theoretical models impose strong feedback in small halos (e.g., Mac Low & Ferrara 1999; Gnedin 2000; Bullock et al. 2001; Stoehr et al. 2002; Kravtsov et al. 2004; Ricotti & Gnedin 2005; Strigari et al. 2008; Sawala et al. 2010; Busha et al. 2010; Sawala et al. 2013). Two processes can dramatically affect the formation and evolution of dwarf-sized halos: heating from the ultraviolet radiation arising from cosmic reionization and feedback from internal supernovae. Both processes are, in principle, capable of completely halting the star formation in a dwarf halo and even fully removing all of the galaxy’s gas. Employing these feedback mechanisms while tying star formation to the collection of baryons has the effect of predicting that essentially all star formation in low-mass halos happens at early times. Both semi-analytic models and hydrodynamical models fail to satisfactorily reproduce the evolution of low mass galaxies in the sense that stellar mass is over-produced per dark matter halo mass. Stars are produced too quickly at early times, resulting in stellar mass fractions that are too high by an order of magnitude. Model galaxies usually do not have the high gas mass fractions commonly observed in present day dwarfs (e.g., Begum et al. 2008), and, as a result, star formation falls off too fast and the colors of simulated dwarf galaxies are too red at  $z = 0$ . This is a manifestation of the “over-cooling” problem which is a challenge for all modeling efforts, but which is exaggerated at low masses.

The missing satellites problem is largest at the lowest masses, and IC 1613 is massive enough that it could be expected to emerge from reionization with its gas intact. Thus, IC 1613 does not provide as strong a test of models for this problem as the other, less massive, galaxies in the LCID sample. However, our deep HST observations have produced SFHs for IC 1613 and Leo A with small uncertainties even at earliest times and have completely ruled out the possibility of an early, dominant phase of star formation. *This represents a real challenge for any model where star formation follows mass assembly.*

### 5.2. Direct Comparison with Models Highlighting the “Over-Cooling” Problem

Sawala et al. (2011) have highlighted the shortcomings of models for dwarf galaxies where star formation

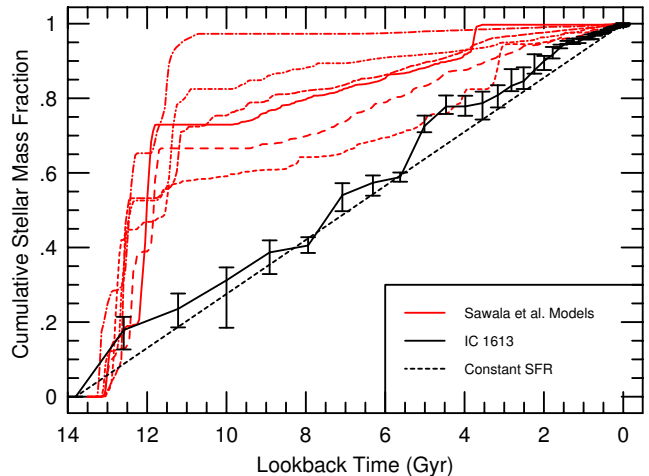


FIG. 11.— Comparison of the SFH of IC 1613 with model SFHs calculated by Sawala et al. (2011). The six model galaxies have halo masses at  $z = 0$  of  $\sim 10^{10} M_{\odot}$ , which is comparable to the estimated halo mass for IC 1613. The difference in the early SFHs between the models and IC 1613 is very clear.

follows directly from mass assembly. They presented a set of high-resolution hydrodynamical simulations of the formation and evolution of isolated dwarf galaxies including the most relevant physical effects, namely metal-dependent cooling, star formation, feedback from Type II and Ia SNe, and UV background radiation. Their results are very useful for a direct comparison with observations. They identify and study six halos with present day dark matter halo masses of  $\approx 10^{10} M_{\odot}$  with stellar masses ranging between  $4.9 \times 10^7 M_{\odot}$  and  $1.0 \times 10^8 M_{\odot}$ . For comparison, IC 1613 has an estimated stellar mass of  $\sim 10^8 M_{\odot}$  (McConnachie 2012), and the observed maximum rotation velocity of  $25 \text{ km s}^{-1}$  (Lake & Skillman 1989). If we associate this peak rotation velocity with the maximum circular velocity of IC 1613’s host dark matter halo, this corresponds to a virial mass<sup>21</sup> of  $M_{\text{vir}} = 3.2 \times 10^9 M_{\odot}$ . This is likely to be a lower limit, however, as the peak of the circular velocity curve for the dark matter halo may be attained at radii beyond the extent of the stellar or gaseous tracers. Abundance matching models find that galaxies with stellar masses of  $10^8 M_{\odot}$  should be hosted by halos with virial masses of  $\sim 3 \times 10^{10} M_{\odot}$  (e.g., Behroozi et al. 2013). Given these estimates, the models of Sawala et al. provide an excellent sample to compare to the derived SFH of IC 1613.

As Figure 11 demonstrates clearly, the early evolution of the model galaxies all depart significantly from that of IC 1613. In essence, the models all have SFRs which depend directly on the gas content of the galaxies. As highlighted by Sawala et al. (2011), since, in the current paradigm, most of the mass of a low mass galaxy is in place well before  $z = 1$  (e.g., Fakhouri et al. 2010), then any prescription in which star formation follows gas content is going to build up most of the stellar mass before  $z = 1$ .

This discrepancy between models and observations, while demonstrated here for IC 1613, is beginning to ap-

<sup>21</sup> Using data from the Millennium-II Simulation (Boylan-Kolchin et al. 2009), we find that:  
 $V_{\text{max}} = 36 \text{ km s}^{-1} (M_{\text{vir}}/10^{10} M_{\odot})^{0.316}$ .

pear to be the norm. Although the numbers are very limited, so far, all gas-rich dwarfs for which there exist sufficiently deep HST observations (i.e., Leo A, Leo T, SMC: Cole et al. 2007; Weisz et al. 2012, 2013) show no evidence for a dominant early episode of star formation.

### 5.3. Potential Solutions for the “Over-Cooling” Problem

There have been various attempts to improve models to better accommodate the inefficient star formation in dwarf galaxies. Stinson et al. (2007) used SPH + N-body simulations and showed that supernova feedback could disrupt enough gas to temporarily quench star formation. Episodic star formation follows from the cycling of gas into a hot halo with subsequent cooling and in-fall. Orban et al. (2008) account for the prolonged star formation observed in dwarfs by adding a stochastic variation in the density threshold of the star formation law. Essentially, this simply reduces the efficiency of star formation by hand, but the result is a significantly improved match to the observed SFHs of dwarfs. Recently, Stinson et al. (2013) have demonstrated that the thermal feedback from early star formation can effectively decouple star formation from mass assembly, thus producing more realistic SFHs.

Gnedin et al. (2009) and Gnedin & Kravtsov (2010, 2011) have proposed a different physical approach by investigating the conversion of atomic to molecular gas and its affect on the efficiency of star formation. This is well motivated by the observational work of Leroy et al. (2008) and Bigiel et al. (2008), which clearly demonstrate that star formation follows the molecular gas content and not the total gas content. In the specific case of dwarf galaxies, Kuhlen et al. (2012) show that models which incorporate a star formation prescription regulated by the local abundance of molecular hydrogen lead to the less efficient star formation that is desired. Unfortunately, their first attempts are not completely successful as they state, “like most cosmological galaxy formation simulations to date, our simulated galaxies suffer from the so-called baryonic overcooling problem, resulting in unrealistically high central densities (and hence strongly peaked circular velocity curves) and stellar mass fractions in our high-mass halos that are too large compared to observations.” However, this appears to be a very promising avenue for future exploration (see also Christensen et al. 2012; Zolotov et al. 2012; Kuhlen et al. 2013).

Starckenburg et al. (2013) used a semi-analytic galaxy formation model to investigate the properties of the satellites of Milky Way-like galaxies and were able to match the star formation histories of several dwarf satellites. The extended SFHs of these satellites were a result of a gas density threshold for star formation. Galaxies could have large reservoirs of gas lying just below the threshold, leading to inefficient star formation (requiring a minor accretion or interaction event).

Shen et al. (2013) have produced new simulations including supernova feedback, a star formation recipe based on a high gas density threshold, metal-dependent radiative cooling, turbulent diffusion of metals and thermal energy, and UV background radiation. They reproduce the observed stellar mass and cold gas content, the SFHs, and the metallicities typical of field dwarfs in the Local Volume. In Figure 12, we reproduce the cumulative stellar mass fraction for four of the model galaxies

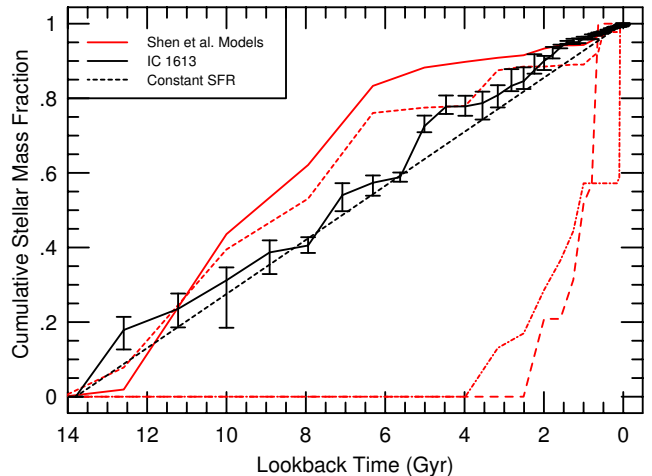


FIG. 12.— Comparison of the SFH of IC 1613 with model SFHs calculated by Shen et al. (2013). The two model galaxies with nearly constant star formation are “Bashful” and “Doc” with halo masses at  $z = 0$  of  $\sim 4 \times 10^{10} M_{\odot}$  and  $\sim 1 \times 10^{10} M_{\odot}$ , respectively, comparable to the estimated halo mass for IC 1613. “Bashful” and “Doc” have nearly constant star formation and lack a dominant early episode of star formation as is observed in IC 1613. The two model galaxies with a delayed onset of star formation are “Dopey” and “Grumpy” with smaller halo masses at  $z = 0$  of  $\sim 3 \times 10^9 M_{\odot}$  and  $\sim 2 \times 10^9 M_{\odot}$ , respectively, (which are considerably less massive than IC 1613, but might be more directly comparable to Leo A).

in Shen et al. (2013). Two of the galaxies (“Bashful” and “Doc”) have virial masses which are comparable to IC 1613. These two models show nearly constant star formation with no dominant early episode of star formation, as observed in IC 1613. In detail, the SFHs of these two models start later and rise faster during intermediate ages. The slower start of the models as compared to that of the measured SFHs may be attributed to differences in how time is defined in the two methods. That is, the simulations start at a fixed, given time, whereas the observationally derived ages come from stellar evolution libraries, and therefore depend on their underlying physics (e.g., nuclear reaction rates).

The two lower mass galaxies (“Dopey” and “Grumpy”) show no early star formation at all, and only start forming stars at intermediate ages. These two models correspond to halo masses significantly less than that of IC 1613, but might be more comparable to that of Leo A (cf. Figure 10). Note, however, that the stellar masses are even more discrepant. That is, Dopey and Grumpy have stellar masses of  $10^5$  and  $5 \times 10^5 M_{\odot}$  compared to  $10^8$  and  $6 \times 10^6 M_{\odot}$  for IC 1613 and Leo A.

Naively, the late onset of star formation in the Dopey and Grumpy models would appear to be in contradiction to observations in which all dwarf galaxies observed to date show evidence for an old ( $\geq 10$  Gyr) population, particularly as evidenced by the presence of RR Lyrae stars. For example, RR Lyrae stars have been observed in Leo A (Dolphin et al. 2002; Bernard et al. 2013). However, Shen et al. (2013) hypothesize that such systems may be the very metal poor systems necessary for the production of extremely metal deficient galaxies such as I Zw 18 (see, e.g., discussion and references in Skillman et al. 2013).

#### 5.4. Other Implications

One of the successes of recent modeling of dwarfs has been the ability of simulations to solve the cusp/core problem for dwarf galaxies (e.g., Governato et al. 2010; Pontzen & Governato 2012; Governato et al. 2012; Teyssier et al. 2013). The dark matter halos of observed dwarf galaxies show nearly constant density cores, while steep central dark-matter profiles are expected from CDM models (e.g., de Blok et al. 2001). The resolution to this conundrum lies in strong outflows from supernovae to remove low-angular-momentum gas from the centers of dwarf galaxies. This solves two problems as bulgeless dwarf galaxies are formed with shallow central dark-matter profiles, and a large fraction of the original baryons are lost from the galaxy, resulting in the lower baryon fractions (relative to the universal fraction) which are observed (e.g., McGaugh et al. 2010).

What is not clear is whether the current ideas concerning how to produce inefficient star formation also lead to cored dark matter halos. Clearly the strong outflows need to occur when the mass assembly is taking place, which is early on. If the vast majority of the star formation is delayed until later times, after the mass assembly is virtually finished, then the central outflow solution to the cusp/core problem may not arise self-consistently. A related point is the energetic requirements for creating bulgeless galaxies and forming cores in state-of-the-art hydrodynamic simulations. Simulations that are currently successful require (1) highly efficient coupling between the energy released in a supernova explosion and the ISM of a galaxy – values typically adopted are 0.4–1 (Governato et al. 2010; Teyssier et al. 2013; Shen et al. 2013) and (2) an artificial prevention of gas cooling for approximately  $10^7$  years in a region surrounding a supernova explosion, meant to capture processes that may occur at sub-grid scales and cannot be directly included in the simulation (Stinson et al. 2006). The success of simulations in producing bulgeless, cored dwarf galaxies with relatively low-level, extended star formation can be therefore seen as predictions for the effective coupling of supernova explosions with the ISM and for the efficacy of additional feedback processes (such as stellar winds) at heating the ISM on small scales. These predictions of very efficient coupling may be confirmed or refuted with future generations of simulations that model the relevant processes directly.

Finally, although we have emphasized the difficulty of producing a nearly constant SFR as seen in IC 1613, observations of dwarf galaxies in the Local Volume point toward a large diversity of SFHs. Determining the critical parameters which drive that diversity is paramount. How can it be that dwarfs with halos of similar mass, which presumably have similar accretion histories and early formation times, have vastly different SFHs? Is environment and interaction history the main driver of the diversity (see, e.g., Sawala et al. 2012; Benítez-Llambay et al. 2013)? From an observational point of view, strong constraints will depend on accurate determinations of the early SFHs of a larger number of galaxies within and beyond the Local Group from both deep photometry as presented here and spectroscopic studies of individual stars (e.g., Kirby et al. 2011; de Boer et al. 2012a,b). Clearly the sample of one presented here, and the very

small number of comparably observed galaxies presents a great limitation to our knowledge of the evolution of dwarf galaxies.

## 6. SUMMARY AND CONCLUSIONS

We have presented the SFH of the dIrr galaxy IC 1613, based on deep HST photometry obtained with the ACS.

- The SFH with relatively small uncertainties has been obtained for the entire lifetime of the galaxy. The solution shows that the SFH of IC 1613 is consistent with a constant SFR over its entire lifetime.
- Most or all the star formation was produced in IC 1613 after the reionization epoch, assumed to occur  $\sim 12.8$  Gyr ago. There is no evidence of an early dominant episode of star formation in IC 1613.
- A comparison of the derived SFH of IC 1613 with the models of Sawala et al. (2011) reinforce their observation that models where star formation follows mass assembly form too many stars too early. This well known aspect of the so called “over-cooling problem” appears to be universal, but now, with the deep HST photometry of IC 1613, we see that the problem reaches back to the very earliest times in the evolution of galaxies.
- There are proposed solutions to the over-cooling problem for dwarf galaxies. The solutions discussed in this paper rely on an efficient coupling of supernova feedback to the ISM. The predictions of very efficient coupling may be confirmed or refuted with future generations of simulations that model the relevant processes directly and through future observations of dwarf galaxy SFHs with similar quality to the LCID studies.

We would like to thank Till Sawala for sharing the numerical results of his modeling, and Greg Stinson, Piero Madau, Alyson Brooks, and the referee for helpful comments. Support for this work was provided by NASA through grant GO-10515 from the Space Telescope Science Institute, which is operated by AURA, Inc., under NASA contract NAS5-26555. Support for DRW is provided by NASA through Hubble Fellowship grant HST-HF-51331.01 awarded by the Space Telescope Science Institute. The computer network at IAC operated under the Condor software license has been used. Authors SH, AA, CG, and MM are funded by the IAC (grant P3/94) and, with SC, PS, and EB, by the Science and Technology Ministry of the Kingdom of Spain (grant AYA2007-3E3507) and Economy and Competitiveness Ministry of the Kingdom of Spain (grant AYA2010-16717). This research has made use of NASA’s Astrophysics Data System Bibliographic Services and the NASA/IPAC Extragalactic Database (NED), which is operated by the Jet Propulsion Laboratory, California Institute of Technology, under contract with the National Aeronautics and Space Administration.

## REFERENCES

- Albert, L., Demers, S., & Kunkel, W. E. 2000, *AJ*, 119, 2780
- Aparicio, A., & Gallart, C. 2004, *AJ*, 128, 1465
- Aparicio, A., & Hidalgo, S. L. 2009, *AJ*, 138, 558
- Aparicio, A., & Tikhonov, N. 2000, *AJ*, 119, 2183
- Aparicio, A., Tikhonov, N., & Karachentsev, I. 2000, *AJ*, 119, 177
- Asplund, M., Grevesse, N., Sauval, A. J., & Scott, P. 2009, *ARA&A*, 47, 481
- Battinelli, P., & Demers, S. 2000, *AJ*, 120, 1801
- Battinelli, P., & Demers, S. 2006, *A&A*, 447, 473
- Bedin, L. R., Cassisi, S., Castelli, F., Piotto, G., Anderson, J., Salaris, M., Momany, Y., & Pietrinferni, A. 2005, *MNRAS*, 357, 1038
- Behroozi, P. S., Wechsler, R. H., & Conroy, C. 2013, *ApJ*, 770, 57
- Begum, A., Chengalur, J. N., Karachentsev, I. D., Sharina, M. E., & Kaisin, S. S. 2008, *MNRAS*, 386, 1667
- Benítez-Llambay, A., Navarro, J. F., Abadi, M. G., et al. 2013, *ApJ*, 763, L41
- Benson, A. J., Bower, R. G., Frenk, C. S., et al. 2003, *ApJ*, 599, 38
- Berg, D. A., Skillman, E. D., Marble, A. R., et al. 2012, *ApJ*, 754, 98
- Bernard, E. J., Aparicio, A., Gallart, C., Padilla-Torres, C. P., & Panniello, M. 2007, *AJ*, 134, 1124
- Bernard, E. J., Monelli, M., Gallart, C., et al. 2010, *ApJ*, 712, 1259
- Bernard, E. J., Monelli, M., Gallart, C., et al. 2013, *MNRAS*, 432, 3047
- Bigiel, F., Leroy, A., Walter, F., et al. 2008, *AJ*, 136, 2846
- Borissova, J., Georgiev, L., Rosado, M., et al. 2000, *A&A*, 363, 130
- Boylan-Kolchin, M., Springel, V., White, S. D. M., Jenkins, A., & Lemson, G. 2009, *MNRAS*, 398, 1150
- Bullock, J.S., Kravtsov, A.V., & Weinberg, D.H. 2001, *ApJ*, 548, 33
- Busha, M. T., Alvarez, M. A., Wechsler, R. H., Abel, T., & Strigari, L. E. 2010, *ApJ*, 710, 408
- Christensen, C., Quinn, T., Governato, F., et al. 2012, *MNRAS*, 425, 3058
- Cole, A. A., Tolstoy, E., Gallagher, J. S., III, et al. 1999, *AJ*, 118, 1657
- Cole, A. A., Skillman, E. D., Tolstoy, E., et al. 2007, *ApJ*, 659, L17
- de Blok, W. J. G., McGaugh, S. S., Bosma, A., & Rubin, V. C. 2001, *ApJ*, 552, L23
- de Boer, T. J. L., Tolstoy, E., Hill, V., et al. 2012, *A&A*, 539, A103
- de Boer, T. J. L., Tolstoy, E., Hill, V., et al. 2012, *A&A*, 544, A73
- Demers, S., Battinelli, P., & Artigau, E. 2006, *A&A*, 456, 905
- Dohm-Palmer, R. C., Skillman, E. D., Saha, A., et al. 1997, *AJ*, 114, 2527
- Dohm-Palmer, R. C., Skillman, E. D., Gallagher, J., et al. 1998, *AJ*, 116, 1227
- Dolphin, A. E. 2000, *PASP*, 112, 1383
- Dolphin, A. E. 2002, *MNRAS*, 332, 91
- Dolphin, A. E. 2012, *ApJ*, 751, 60
- Dolphin, A. E. 2013, *ApJ*, 775, 76
- Dolphin, A. E., Saha, A., Skillman, E. D., et al. 2001, *ApJ*, 550, 554
- Dolphin, A. E., Saha, A., Claver, J., et al. 2002, *AJ*, 123, 3154
- Dolphin, A. E., Weisz, D. R., Skillman, E. D., & Holtzman, J. A. 2005, *arXiv:astro-ph/0506430*
- Dotter, A., Chaboyer, B., Jevremović, D., Baron, E., Ferguson, J. W., Sarajedini, A., & Anderson, J. 2007, *AJ*, 134, 376
- Duane, S., Kennedy, A. D., Pendleton, B. J., & Roweth, D. 1987, *PhLB*, 195, 216
- Fakhouri, O., Ma, C.-P., & Boylan-Kolchin, M. 2010, *MNRAS*, 406, 2267
- Fan, X., Strauss, M. A., Becker, R. H., et al. 2006, *AJ*, 132, 117
- Ford, H. C., et al. 1998, *Proc. SPIE*, 3356, 234
- Gallagher, J. S., III, Hunter, D. A., & Tutukov, A. V. 1984, *ApJ*, 284, 544
- Gallagher, J. S., Tolstoy, E., Dohm-Palmer, R. C., et al. 1998, *AJ*, 115, 1869
- Gallart, C., Zoccali, M., & Aparicio, A. 2005, *ARA&A*, 43, 387
- Gallart, C., Stetson, P. B., Meschin, I. P., Pont, F., & Hardy, E. 2008, *ApJ*, 682, L89
- Girardi, L., Williams, B. F., Gilbert, K. M., et al. 2010, *ApJ*, 724, 1030
- Gnedin, N. Y. 2000, *ApJ*, 542, 535
- Gnedin, N. Y., Tassis, K., & Kravtsov, A. V. 2009, *ApJ*, 697, 55
- Gnedin, N. Y., & Kravtsov, A. V. 2010, *ApJ*, 714, 287
- Gnedin, N. Y., & Kravtsov, A. V. 2011, *ApJ*, 728, 88
- Governato, F., Brook, C., Mayer, L., et al. 2010, *Nature*, 463, 203
- Governato, F., Zolotov, A., Pontzen, A., et al. 2012, *MNRAS*, 422, 1231
- Grocholski, A. J., van der Marel, R. P., Aloisi, A., et al. 2012, *AJ*, 143, 117
- Hidalgo, S. L., Aparicio, A., & Gallart, C. 2008, *AJ*, 136, 2332
- Hidalgo, S. L., Marín-Franch, A., & Aparicio, A. 2003, *AJ*, 125, 1247
- Hidalgo, S. L., Aparicio, A., Martínez-Delgado, D. & Gallart, C. 2009, *ApJ*, 705, 704
- Hidalgo, S. L., Aparicio, A., Skillman, E., et al. 2011, *ApJ*, 730, 14
- Hidalgo, S. L., Monelli, M., Aparicio, A., et al. 2013, *ApJ*, 778, 103
- Hill, J.R. et al. 1998, *ApJ*, 496, 648
- Holtzman, J. A., Burrows, C. J., Casertano, S., et al. 1995, *PASP*, 107, 1065
- Holtzman, J. A., Afonso, C., Dolphin, A. 2006, *ApJS*, 166, 534
- Hopkins, A. M. 2004, *ApJ*, 615, 209
- Kauffmann, G., White, S. D. M., & Guiderdoni, B. 1993, *MNRAS*, 264, 201
- Kallivayalil, N., van der Marel, R. P., Besla, G., Anderson, J., & Alcock, C. 2013, *ApJ*, 764, 161
- Kirby, E. N., Lanfranchi, G. A., Simon, J. D., Cohen, J. G., & Guhathakurta, P. 2011, *ApJ*, 727, 78
- Kirby, E. N., Bullock, J. S., Boylan-Kolchin, M., Kaplinghat, M., & Cohen, J. G. 2014, *MNRAS*, 439, 1015
- Klypin, A., Kravtsov, A.V., Valenzuela, O., & Prada, F. 1999, *ApJ*, 522, 82
- Komatsu, E., Dunkley, J., Nolte, M.R., Bennett, C.L., Gold, B., et al. 2009, *ApJS*, 180, 330
- Kravtsov, A.V., Gnedin, O.Y., & Klypin, A.A. 2004, *ApJ*, 609, 482
- Kuhlen, M., Krumholz, M. R., Madau, P., Smith, B. D., & Wise, J. 2012, *ApJ*, 749, 36
- Kuhlen, M., Madau, P., & Krumholz, M. R. 2013, *ApJ*, 776, 34
- Lake, G., & Skillman, E. D. 1989, *AJ*, 98, 1274
- Lee, H., Grebel, E. K., & Hodge, P. W. 2003, *A&A*, 401, 141
- Leisy, P., Corradi, R. L. M., Magrini, L., Greimel, R., Mampaso, A., & Dennefeld, M. 2005, *A&A*, 436, 437
- Leroy, A. K., Walter, F., Brinks, E., et al. 2008, *AJ*, 136, 2782
- Mac Low, M.-M., & Ferrara, A. 1999, *ApJ*, 513, 142
- Madau, P., Pozzetti, L., & Dickinson, M. 1998, *ApJ*, 498, 106
- Magrini, L., Corradi, R. L. M., Greimel, R., et al. 2003, *A&A*, 407, 51
- Mateo, M. L. 1998, *ARA&A*, 36, 435
- McConnachie, A. W. 2012, *AJ*, 144, 4
- McGaugh, S. S., Schombert, J. M., de Blok, W. J. G., & Zagursky, M. J. 2010, *ApJ*, 708, L14
- Monelli, M., Cassisi, S., Bernard, E. J., Hidalgo, S. L., Aparicio, A., Gallart, C., & Skillman, E. D. 2010a, *ApJ*, 718, 707
- Monelli, M., et al. 2010b, *ApJ*, 720, 1225
- Monelli, M., et al. 2010c, *ApJ*, 722, 1864
- Moore, B., Ghigna, S., Governato, F., et al. 1999, *ApJ*, 524, L19
- Noël, N. E. D., Aparicio, A., Gallart, C., Hidalgo, S. L., Costa, E., & Méndez, R. A. 2009, *ApJ*, 705, 1260
- Orban, C., Gnedin, O. Y., Weisz, D. R., et al. 2008, *ApJ*, 686, 1030
- Pietrinferni, A., Cassisi, S., Salaris, M., & Castelli, F. 2004, *ApJ*, 612, 168
- Pontzen, A., & Governato, F. 2012, *MNRAS*, 421, 3464
- Ricotti, M., & Gnedin, N.Y. 2005, *ApJ*, 629, 259
- Ryś, A., Grocholski, A. J., van der Marel, R. P., Aloisi, A., & Annibali, F. 2011, *A&A*, 530, A23
- Sawala, T., Scannapieco, C., Maio, U., & White, S. 2010, *MNRAS*, 402, 1599
- Sawala, T., Guo, Q., Scannapieco, C., Jenkins, A., & White, S. 2011, *MNRAS*, 413, 659

- Sawala, T., Scannapieco, C., & White, S. 2012, MNRAS, 420, 1714
- Sawala, T., Frenk, C. S., Crain, R. A., et al. 2013, MNRAS, 431, 1366
- Shen, S., Madau, P., Conroy, C., Governato, F., & Mayer, L. 2013, arXiv:1308.4131
- Sirianni, M., et al. 2005, PASP, 117, 1049
- Skillman, E. D., Kennicutt, R. C., & Hodge, P. W. 1989, ApJ, 347, 875
- Skillman, E. D., Bomans, D. J., & Kobulnicky, H. A. 1997, ApJ, 474, 205
- Skillman, E.D., Tolstoy, E., Cole, A.A., Dolphin, A.E., Saha, A., Gallagher, J.S., Dohm-Palmer, R.C., & Mateo, M. 2003a, ApJ, 596, 253
- Skillman, E. D., Côté, S., & Miller, B. W. 2003b, AJ, 125, 593
- Skillman, E. D., Salzer, J. J., Berg, D. A., et al. 2013, AJ, 146, 3
- Spergel, D. N., et al. 2007, ApJS, 170, 377
- Starkenburger, E., Helmi, A., De Lucia, G., et al. 2013, MNRAS, 429, 725
- Stetson, P. B. 1994, PASP, 106, 250
- Stinson, G., Seth, A., Katz, N., et al. 2006, MNRAS, 373, 1074
- Stinson, G. S., Dalcanton, J. J., Quinn, T., Kaufmann, T., & Wadsley, J. 2007, ApJ, 667, 170
- Stinson, G. S., Brook, C., Macciò, A. V., et al. 2013, MNRAS, 428, 129
- Stoehr, F. White, S.D.M., Tormen, G. & Springel, V. 2002, MNRAS, 335, L84
- Strigari, L.E., Bullock, J.S., Kaplinghat, M., Simon, J.D., Geha, M., Willman, B., & Matthew, G. 2008, Nature, 454, 1096
- Tammann, G. A., Reindl, B., & Sandage, A. 2011, A&A, 531, A134
- Teyssier, R., Pontzen, A., Dubois, Y., & Read, J. I. 2013, MNRAS, 429, 3068
- Tolstoy, E., Gallagher, J. S., Cole, A. A., et al. 1998, AJ, 116, 1244
- Tolstoy, E., Hill, V., & Tosi, M. 2009, ARA&A, 47, 371
- van den Bergh, S. 2000, "The galaxies of the Local Group," Cambridge Astrophysics Series Series, vol no: 35, Cambridge University Press
- Weinmann, S. M., Pasquali, A., Oppenheimer, B. D., et al. 2012, MNRAS, 426, 2797
- Weisz, D. R., Dalcanton, J. J., Williams, B. F., et al. 2011, ApJ, 739, 5
- Weisz, D. R., Zucker, D. B., Dolphin, A. E., et al. 2012, ApJ, 748, 88
- Weisz, D. R., Dolphin, A. E., Skillman, E. D., et al. 2013, MNRAS, 431, 364
- Weisz, D. R., Dolphin, A. E., Skillman, E. D., et al. 2014, ApJ, submitted
- Young, L. M., Skillman, E. D., Weisz, D. R., & Dolphin, A. E. 2007, ApJ, 659, 331
- Zaggia, S., Held, E. V., Sommariva, V., et al. 2011, EAS Publications Series, 48, 215
- Zolotov, A., Brooks, A. M., Willman, B., et al. 2012, ApJ, 761, 71